Abstract

Turnouts are a key element of the railway system. They are also one part of the railway system with the highest number of degradation modes and failures for a number of reasons, including dynamic loads generated from non-linearities in the rail geometry and track support stiffness. It is therefore necessary to optimise the performance of the system in terms of its dynamic behaviour taking into account effects on long-term term damage evolution. The main aim of this study is to optimise the rail-pad stiffness in the crossing panel in order to achieve a decrease in the main indicator for ballast settlement, which is ballast pressure. A three-dimensional vehicle/track interaction model has been established, considering a detailed description of the crossing panel support structure. Genetic algorithm has been applied to find the optimum rail-pad combination for a specific case where variation in travelling speed and support conditions have been considered.

Keywords: crossing panel, rail-pad stiffness, design optimisation, vehicle/track interaction.

1 Introduction

Switches and crossings (S&C) play an essential role in the traffic operation of rail networks as they provide flexibility to the system in terms of feasible routes. Even though, these components introduce discontinuities in track geometry. This leads to high impact forces and therefore, turnouts are one of the parts of the railway system with the highest number of failures [1]. In addition, there is a significant longitudinal variation of the vertical support stiffness along the switch and the crossing panel, which contributes to further vibrations and acceleration in the degradation processes of the track. This change of characteristics may be partially controlled by choosing

appropriate support stiffness elements in order to obtain an overall rigidity as smooth as possible through the S&C.

This problem has been partially addressed in the past. For example, in [2] a methodology to optimise support stiffness at the switch panel has been proposed, leading to a significant reduction in the wear indices. In the crossing panel, on the contrary, the support stiffness is briefly analysed, acknowledging high potential for the reduction of material degradation of the crossing nose. In [3], three design parameters, that are the stiffness and the damping of rail-pads and the sleeper's weight, have been considered to optimize the crossing performance in terms of vertical dynamic forces, which are responsible for rolling contact fatigue (RCF) related damage of the crossing nose and wing rails. Under sleeper pads (USPs) are also considered in the paper to help reduce the dynamic impact loads.

Currently, there are no specifications or suggestions on rail-pad stiffness to be installed in the crossing panel depending on the type of support and the type of line, even if it is believed that the track stiffness plays an important role on both the short- and long-term behaviour. Therefore, the main aim of this work is to understand the mayor degradation mechanisms and to propose a new standardization.

In the present study, a genetic algorithm is applied to find an optimum design solution in terms of support stiffness. The objective function is based on damage levels that account for RCF, wear, settlement and fatigue in the components. A three-dimensional vehicle/track interaction model has been developed and used to calculate the dynamic behaviour at the crossing panel. An on-line wheel/rail contact algorithm based on Hertzian theory and Kalker linear creep law is adopted. Additionally the proposed methodology includes an accurate finite element model of the track, which is often neglected in commercial packages. The optimisation process also considers different vehicle speeds and support stiffness.

2 Modelling the vehicle/track interaction at the crossing panel

A representation of the vehicle/track interaction model in the y-z plane used in the present study is shown in Figure 1

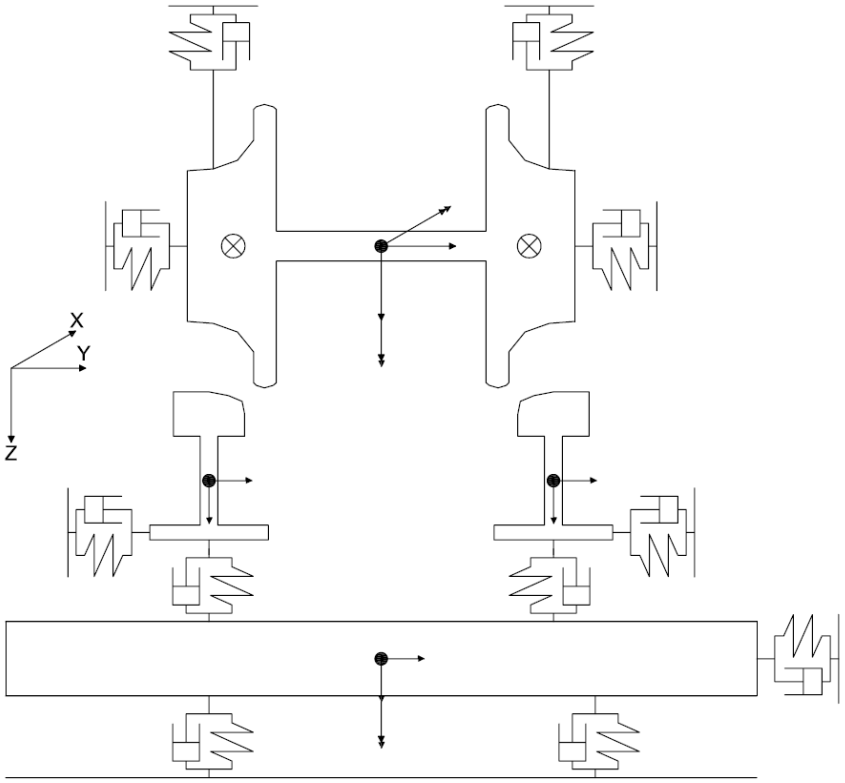

Figure 1: Vehicle/track interaction model in the y-z plane.

A detailed description of each sub-system is given in the following sections: the track model in paragraph 2.1, the vehicle model in paragraph 2.2 and the contact model in paragraph 2.3. Finally, the main input data used is listed in paragraph 2.4.

2.1 Track model

The three-dimensional track model is shown in Figure 2.

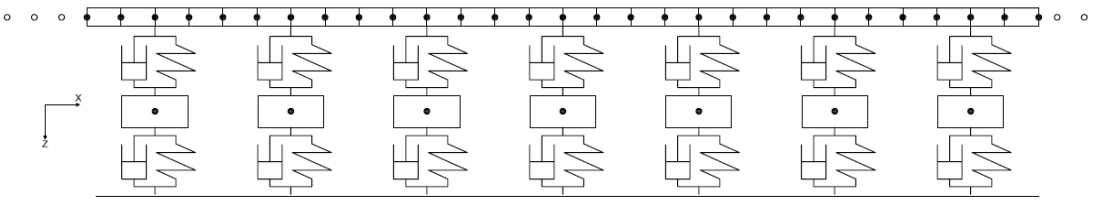

(a)

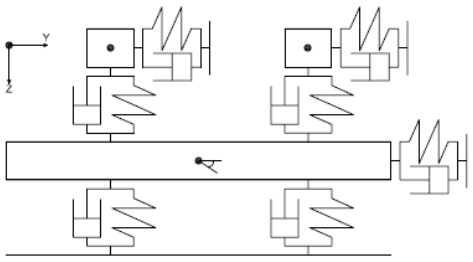

(b)

Figure 2: Track model ((a): x-z plane; (b): y-z plane).

The track is modelled as a two-layer discretely supported ballasted track, including the rail-pad and the sleeper support resilient layers.
Each rail is modelled as a Timoshenko beam. In fact, the Euler-Bernoulli beam theory is not adequate for representation of the rail response to vertical excitation frequencies above 500 Hz [4]. Each node has four degree of freedom (DOFs): vertical and lateral displacement and rotations around the y and z axes. In order to obtain accurate results and capture correctly the abrupt change in the geometrical properties, four beam elements are considered within each sleeper-spacing [5].
The sleepers are modelled as rigid body with 3 DOFs: vertical and lateral displacement and roll rotation. The dynamic response due to forces at the railhead is well represented up to 1 kHz [4]. The effect of sleeper flexibility will be investigated in a future work.

2.2 Vehicle model

A rigid single axle with primary suspensions is considered and the weight of the vehicle is applied as external force. Four DOFs are considered: vertical and lateral displacements; roll and yaw rotations. Each component of the primary suspension (i.e. vertical, lateral and longitudinal component) connects the axle to the ground and is modelled with a linear spring-damper. Bogie steering effects are thus ignored.

2.3 Contact model

The contact element used takes into account the normal and tangential forces present at the wheel-rail interface. The normal forces are modelled using the non-linear Hertzian theory and the tangential forces using the linear Kalker theory [6], corrected according to Shen, Hedrick and Elkins theory [7].

An on-line approach to is used calculate the contact data (i.e. contact angle, rolling radius, point of contact and curvature of the wheel and rail profiles).The on-line approach is more suitable then using contact tables when there is a significant variation of the rail cross-sections along the longitudinal direction

An iterative procedure has been used to solve the non-linear contact problem (Figure 3).

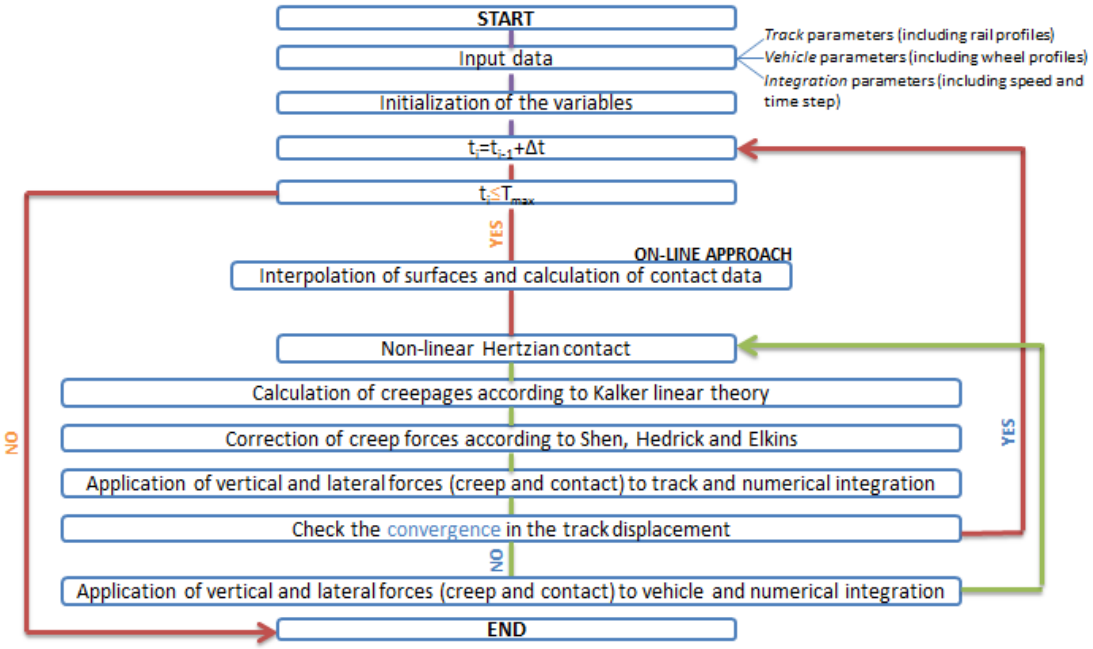

Figure 3: Iterative procedure to solve the non-linear contact problem.

2.4 Input data

The main track data is:

- *Crossing type*: CEN56 1 in 9.25 acute crossing (Figure 4);
- *Rail type*: 56E1 vertical profile;
- *Check rail*: CEN33C1 profile;
- *Sleeper type*: concrete sleepers. The mass and the roll inertia are variable between circa 410 kg and 470 kg as the length is not constant;
- *Sleeper spacing*: 0.6 m.
- *Sleeper support stiffness:* vertical stiffness as below, lateral equal to 37 MN/m.

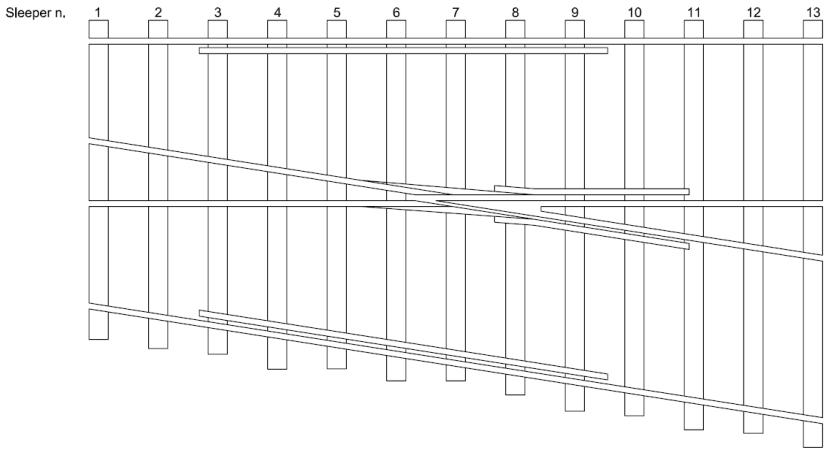

Figure 4: Sketch of the crossing layout (not in scale).

The main vehicle data is:

- *Unsprung mass*: 1500 kg (typical of a freight wagon);
- *Axle load*: 22.5 t;
- *Longitudinal and lateral primary suspension stiffness*: 3.6 MN/m;
- *Vertical primary suspension stiffness*: 5 MN/m.

The main contact data is:

- *Wheel profile*: new, medium worn and heavily worn P10 (typical of a freight wagon);
- *Coefficient of friction*: 0.35;
- *Flange back spacing*: 1.36 m.

Different conditions in terms of vehicle speed and support stiffness are considered, as following:

- *Vehicle speed*: 40/80/120 km/h;
- *Support stiffness*: 50/100/250 MN/m (typical of low, medium and high support quality [8]).

3 Optimization process

The flow chart of the optimisation process used in the present study is shown in Figure 5.

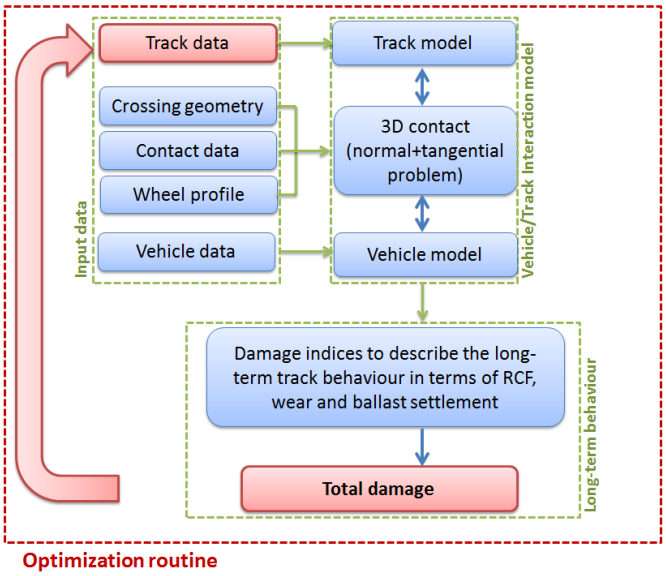

Figure 5: Flow chart of the optimization process.

The optimum solution that minimises the total damage due the passage of a train over the crossing panel is found through a genetic algorithm changing the rail-pad stiffness. The variables used as well as the range considered are presented in Paragraph 3.1.1, the objective function is defined in Paragraph 3.1.2 and finally, the constraints applied are listed in Paragraph 3.1.3.

3.1.1 Variables

Two main variables (X_1 and X_2) are used for the optimisation. They represent the rail-pad stiffness of the load transfer area and of the bearers next to the transfer area respectively (Figure 6).

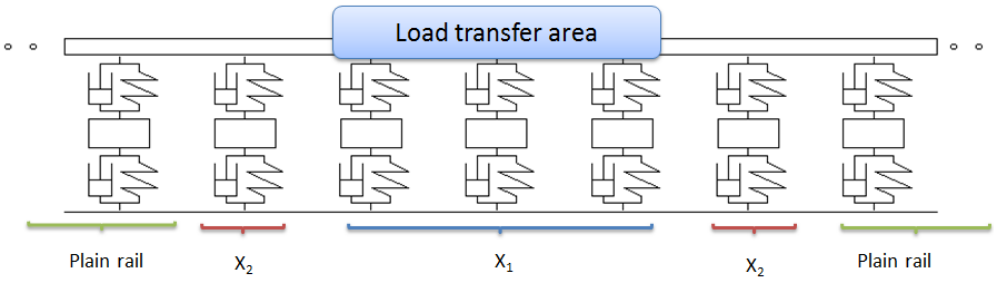

Figure 6: Optimisation variables (X_1 and X_2).

The range considered for both variables is (expressed in MN/m):

$$X_{possible} = [20,100,200,300,500,750,1000] \quad (1)$$

The adopted range is based on typical values for commercial soft and medium/hard railway pads [9].

The three point of control are the nodes above sleeper n.2, n.5 and n.7 (Figure 4). These points have been chosen as the first one represents the first support for the plain rail, the second one is in correspondence of variable X_2 and the third one in correspondence of the crossing nose (variable X_1).

3.1.2 Objective function

Long-term behaviour of the system is assessed through macro indices which can give an indication of the degradation severity, velocity and location. Four main degradation modes are considered: settlement of the ballast layer, wear and rolling contact fatigue (RCF) for the rails and fatigue in the track components as they are the most common causes of failures.

- **Settlement**

According to the literature (for example, [10-12]), the main drivers of the ballast settlement are sleeper accelerations and ballast pressure.

- **Wear and RCF**

In this study, excessive RCF and excessive wear are considered. These concepts are explained in Figure 7.

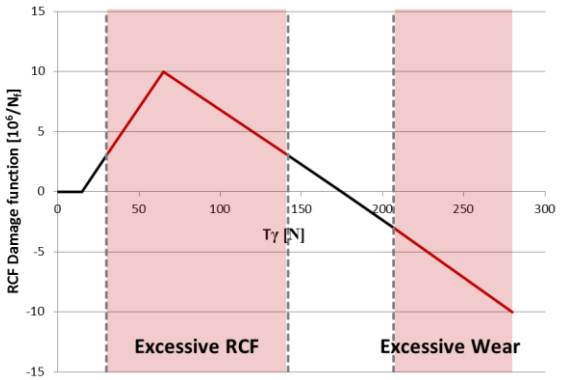

Figure 7: Excessive RCF and excessive wear.

In particular, RCF is considered excessive when the damage function is greater than $3 \cdot 10^6/N_f$, that is when the Tγ values are in the range between 30 N and 142 N. The wear is considered excessive when the damage function is lower than $-3 \cdot 10^6/N_f$, that is when the Tγ values are greater than 207 N. Note that the above damage function was validated against normal grades of rail steel for plain line and on UK routes [13]. Change of material type and application to S&C might in practice necessitate a modified damaged function with is currently not available.

- **Fatigue in the components**

Three main factors are considered:

- *Bending stresses on the rail head*;
- *Bending stresses on the rail foot*, which can lead to transversal crack on the crossing bottom in combination with corrosion and defects;
- *Forces in the rail-pad*, which are an indicator of potential rail-pads and fastening failures.

Therefore, the optimisation problem can be written as follows:

$$\min_{x \in X_{possible}} F(x) \tag{2}$$

Where:
x = vector of the rail-pad stiffness (Paragraph 3.1.1) [MN/m];
$X_{possible}$ = range of possible values for the rail-pad stiffness (Paragraph 3.1.1) [MN/m];
$F(x)$ = objective function:

$$F(x) = \alpha \cdot \sum_{i=1}^{n_w} w_i \cdot \left(\frac{SA}{SA^*} - 1\right) + \beta \cdot \sum_{i=1}^{n_w} w_i \cdot \left(\frac{BP}{BP^*} - 1\right) + \gamma \cdot \sum_{i=1}^{n_w} w_i \cdot \left(\frac{Tgamma_{RCF}}{Tgamma_{RCF}^*} - 1\right) + \delta \cdot \sum_{i=1}^{n_w} w_i \cdot \left(\frac{Tgamma_{wear}}{Tgamma_{wear}^*} - 1\right) + \varepsilon \cdot \sum_{i=1}^{n_w} w_i \cdot \left(\frac{Stress_{head}}{Stress_{head}^*} - 1\right) + \theta \cdot \sum_{i=1}^{n_w} w_i \cdot \left(\frac{Stress_{foot}}{Stress_{foot}^*} - 1\right) + \varphi \cdot \sum_{i=1}^{n_w} w_i \cdot \left(\frac{Force_{pad}}{Force_{pad}^*} - 1\right) \tag{3}$$

Where:
$\alpha, \beta, \gamma, \delta, \varepsilon, \theta, \varphi$ = weight per each degradation mode considered;
n_w = number of wheels considered (in this study equal to 3);
w_i = weight of the i-th wheel (0.3 for the new wheel, 0.5 for the medium worn wheel, 0.2 for the heavily worn wheel);
SA, SA^* = maximum sleeper acceleration at the three point of control and maximum sleeper acceleration at the three point of control in the nominal situation [m/s^2];
BP, BP^* = maximum ballast pressure at the three point of control and maximum ballast pressure at the three point of control in the nominal situation [MPa];
$Tgamma_{RCF}$, $Tgamma_{RCF}^*$ = damage function due to excessive RCF and damage function due to excessive RCF in the nominal situation;
$Tgamma_{wear}$, $Tgamma_{wear}^*$ = damage function due to excessive wear and damage function due to excessive wear in the nominal situation;
$Stress_{head}$, $Stress_{head}^*$ = stress on the rail head and stress on the rail head in the nominal situation [MPa];
$Stress_{foot}$, $Stress_{foot}^*$ = stress on the rail foot and stress on the rail foot in the nominal situation [MPa];
$Force_{pad}$, $Force_{pad}^*$ = maximum rail-pad forces at the three point of control and maximum rail-pad forces at the three point of control in the nominal situation [kN].

The location of points of control is explained in the previous section. The nominal situation is the one for which both variables equal to the rail-pad stiffness of the plain rail (i.e. 200 MN/m).

Note that the evolution of the crossing shape over time due to the wear and plastic deformation is out of the scope of the present study. Also, the geometry used is a new geometry and does not vary during the simulations.

3.1.3 Constraints

It is necessary to guarantee that the change in the overall track stiffness is as smooth as possible in order to minimise the impact forces, as illustrated in Figure 8.

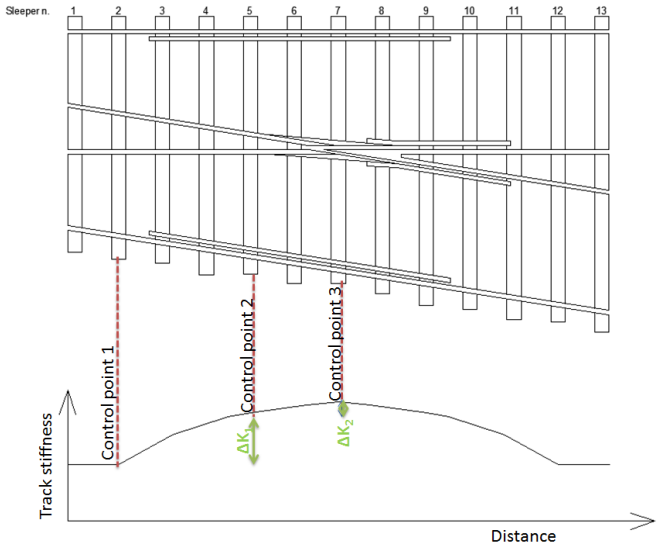

Figure 8: Desirable variation in the track stiffness along the crossing panel.

Therefore, the variation in track stiffness between the first and the second control point should be within the range 30% to 70%, while the variation between the second and the third control point between 20% and 50%:

$$30\% \leq \Delta K_1 \leq 70\% \tag{4}$$

$$20\% \leq \Delta K_2 \leq 50\% \tag{5}$$

Where:
ΔK_1 = percentage difference in the overall track stiffness between the first and the second control point [%];
ΔK_2 = percentage difference in the overall track stiffness between the second and the third control point [%];

The overall track stiffness is calculated performing a static analysis at each control point.

4 Results

4.1.1 Understanding the objective function

In Figure 9, the trend of each key indicator term included in the objective function (Eq. 4) is analysed in detail for the case with low travelling speed (40 km/h) and medium support stiffness (100 MN/m).

It is worth underlying that the following discussions do not take in consideration the constraints.

From a first analysis, it is possible to notice how all the key indicators analysed have different trends, sometimes in antithesis. Furthermore, the level of change of the key indicators varies significantly with the parameter considered, ranging between 10% and 250%. Therefore, a normalisation is necessary when all the terms considered are summed. This is out of the scope of this paper and it will be assessed as part of further works.

Looking in more detail, the following considerations can be drawn:

- **Settlement**
  - *Sleeper acceleration*: Changing the rail-pad stiffness in the crossing panel leads only to an increase of the level of sleeper acceleration. Using very soft pads for both variables leads to an increase of ca. 77% and using very stiff pads for both variables leads to an increase of about 130%. The worst combination of pad stiffness is using very stiff pads under the load transfer area and very soft in the transition, leading to an increment of the sleeper acceleration of ca. 180% w.t.r. of the nominal case.
  - *Ballast pressure*: It is possible to identify a general decrease of ballast pressure with decreasing pad stiffness, as expected. The best combination is using the softest pads available all along the crossing panel, gaining a considerable 15% improvement w.r.t. the nominal case. In practise, this combination is not used due to other considerations including dynamic performance of the vehicle and excessive bending stresses con the foot.
- **Wear/RCF**
  - *Wear*: In the case analysed, there is no excessive wear and confirms that the rail pad properties has little effect on this quantity.
  - *RCF*: The RCF plot shows that this degradation mechanism decreases with decreasing pad stiffness. The best combination is using the softest pads available all along the crossing panel, gaining a relevant 13% improvement w.r.t. the nominal case.
- **Fatigue in the components**
  - *Rail-pad forces*: Apart from some isolated cases, there is a general decrease of forces in the rail-pads with decreasing pad stiffness, as

expected. The best combination is using the softest pads available, gaining a 20% improvement w.r.t. the nominal case.

- *Stresses on the rail foot*: On the contrary of the rail-pad forces, there is a general decrease of stresses with increasing pad stiffness, as the rail is less free to deform. The best combination is using the stiffest pads available, gaining a negligible 5% improvement w.r.t. the nominal case.
- *Stresses on the rail head*: The trend is similar to the foot stresses one.

In Table 1 a brief summary of the findings described in this section is presented.

Degradation mode	Indicator	Best solution	Improvement (w.r.t. nominal case)
Settlement	Sleeper acceleration	Nominal case	0%
	Ballast pressure	Soft pads	15%
Wear/RCF	Wear	-	-
	RCF	Soft pads	13%
Fatigue in the components	Rail-pad forces	Soft pads	20%
	Stresses on the rail foot	Stiff pads	5%
	Stresses on the rail head	Stiff pads	5%

Table 1: Summary of findings in terms of best solution and maximum improvement achievable per each indicator considered.

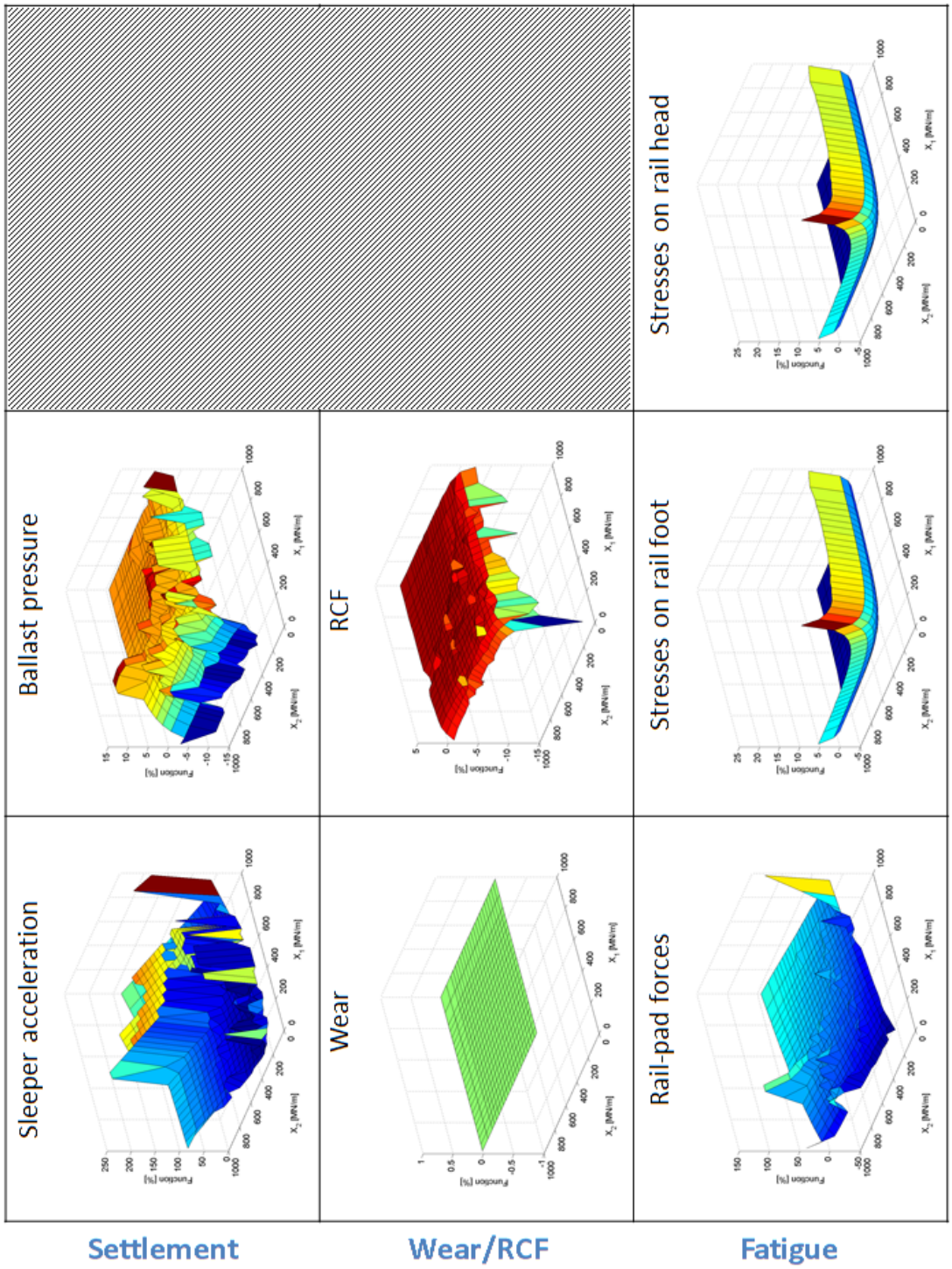

Figure 9: Trend of each term included in the objective function.

4.1.2 Minimising the ballast degradation mode

Due to the complexity of the objective function, only the optimisation of the rail-pad stiffness to reduce the ballast pressure is considered further in this study. In fact, it is

reasonable to assume that this is the most expensive degradation mode amongst the four considered (e.g. settlement, wear, RCF, fatigue) in terms of maintenance and renewal costs. In addition, a constraint to limit the maximum stress on the rail foot has been applied as follows:

$$\frac{\sigma_{foot}}{\sigma_{foot,y}} \leq 70\% \quad (6)$$

Where:
σ_{foot} = maximum stress on the rail foot [MPa];
$\sigma_{foot,y}$ = yield stress on the rail foot, equal to 850 [MPa]. This value is an approximate value depending on the material used in the crossing, that is the manganese.

The same case considered in the previous section (i.e. low speed and medium support stiffness) is analysed in detail.

Figure 10 shows both the value of the objective function and the value of the two parameters at each iteration.

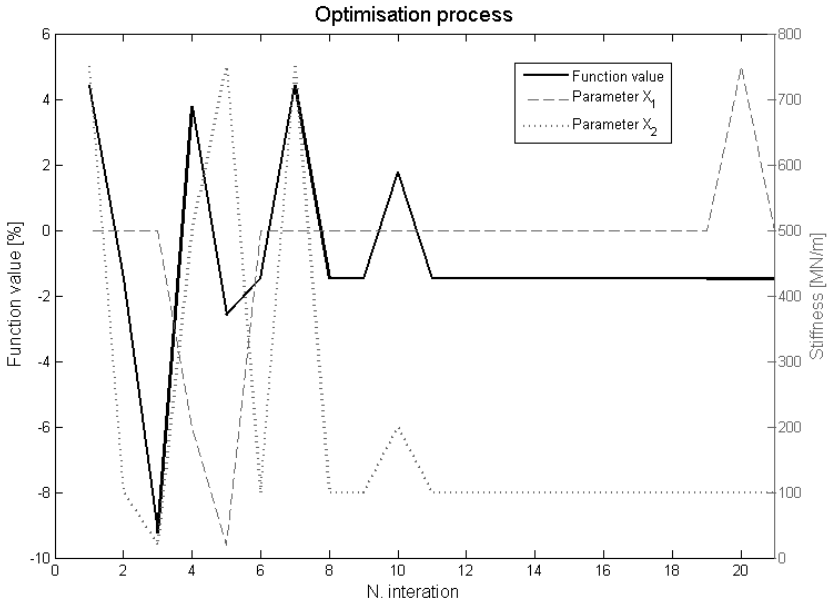

Figure 10: Optimisation process (parameter X_1: dashed grey line; parameter X_2: dotted grey line; function value: black line).

The function value experiences high oscillations in the first seven iterations, from ca. 4% to ca. -9.5% (Figure 10, black line). Then, it stabilises after the tenth iteration around a reduction of ca. -1.5%.

It is worth noticing that the maximum reduction shown in the plot (ca. -9.5%) is not a feasible solution as the correspondent two parameters X_1 and X_2 (Figure 10, dashed and dotted grey lines) do not comply the constraint about the overall track stiffness.

The values of the parameters considered during the optimisation process are also plotted in the ballast pressure surface (Figure 11).

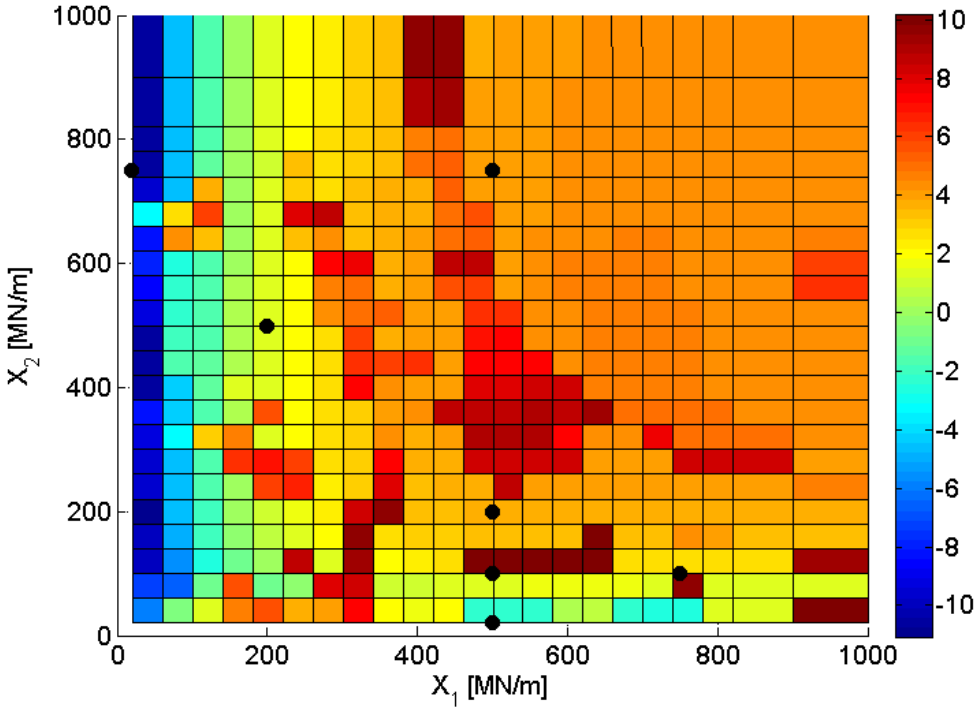

Figure 11: Values of the parameters considered during the optimisation process plotted in the ballast pressure surface.

Figure 12 shows the rail inertia, the rail-pad stiffness distribution for the optimum solution found and the total track stiffness, which is calculated in correspondence of the three control points (Paragraph 3.1.2).

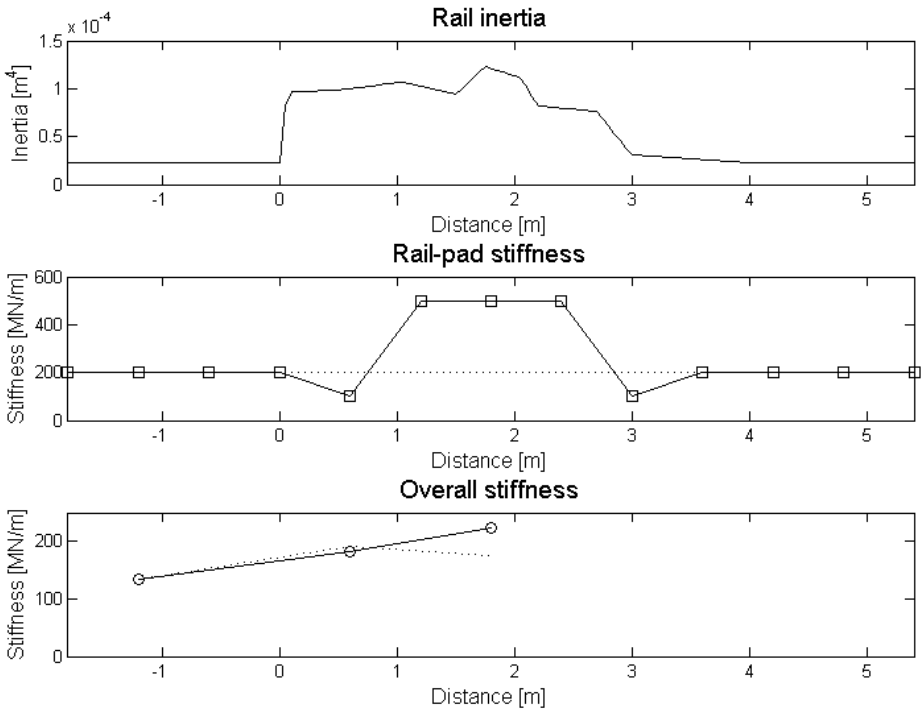

Figure 12: Track stiffness for the optimum solution.

Figure 12 clearly demonstrates how the optimum solution found by the genetic algorithm smooths the overall support characteristics leading to the desirable parabolic configuration (Figure 8).

In Figure 13 the results of the optimisation process in terms of maximum reduction in ballast pressure versus support stiffness for different speed are shown.

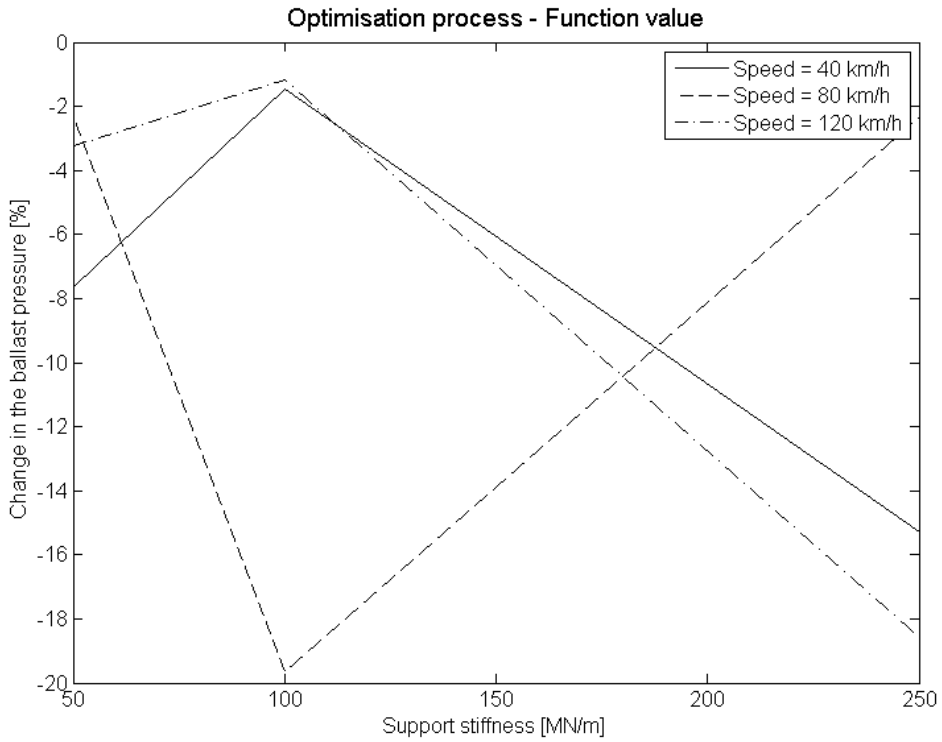

Figure 13: Results of the optimisation process in terms of maximum reduction in ballast pressure versus support stiffness for different speed.

In case of low speed (Figure 13, continuous line), the maximum reductions are circa 7.5% in case of low/medium quality of the support stiffness. Increasing the support stiffness up to 250 MN/m, there are further reductions of the ballast pressure w.r.t. of the baseline scenario, up to circa 15%.

Increasing the speed to 80 km/h (Figure 13, dashed line), the maximum change is obtained in correspondence of the medium support stiffness, with a remarkable 20% reduction. In case of very low and very high support conditions, the maximum reduction is almost negligible (ca. 2.5%). This parabolic behaviour can be explained with the non-linear dynamic effects induced by the train passing over the crossing.

Finally, in correspondence of the highest speed considered (Figure 13, dashed and dotted line), the trend is similar to the case of the lowest speed considered. In fact, for soft/medium support, the maximum reduction is circa 3% on average and it increases to circa 18% in case of stiff support.

In Figure 14, the optimum pad stiffness per each speed class and each support class is summarised.

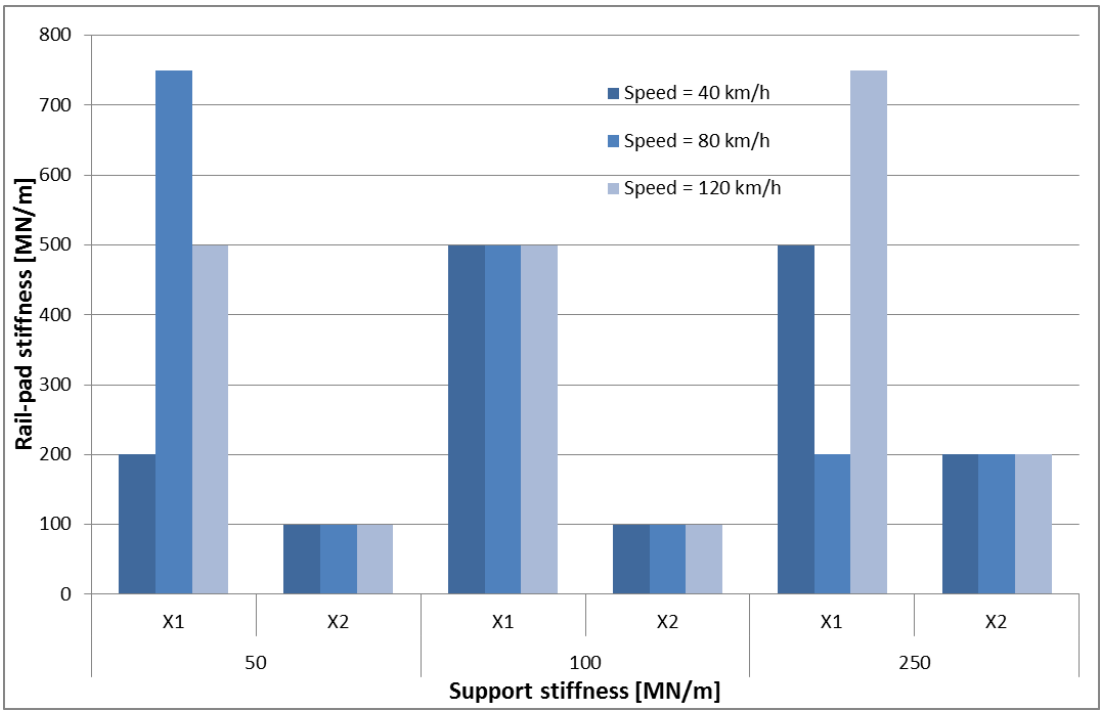

Figure 14: Optimum pad stiffness per each speed class and each support class.

Considering only the parameter X_1 in **Error! Reference source not found.**, as the other parameter is directly linked to it, it is possible to notice that for low and high speed (i.e. 40 and 120 km/h) the optimum pad stiffness is increasing for increasing support quality, whereas for the medium speed (i.e. 80 km/h) the optimum value is decreasing for increasing support quality. Moreover, if the line type is slow, it is possible to use soft/medium pads, while if the speed increases it is better to use medium pads.

To conclude, the results show that there are benefits to have stiff pads under the load transfer area and slightly softer ones at the edges of the crossing panel, especially in case of medium/good support. This tends to change with speed as the track support stiffness becomes poorer, as non-linear behaviour is occurring.

5 Conclusions and further works

This paper presents a methodology to optimise the rail-pad stiffness in the crossing panel minimising the most common degradation modes and guaranteeing a smooth distribution of total track stiffness. A three-dimensional vehicle/track interaction model has been used in order to evaluate the dynamic behaviour of a single axle negotiating the crossing panel. The proposed model includes an accurate description of the track, which is often neglected in commercial vehicle dynamics simulations studies.

The contribution of each indicator considered in the objective function is analysed in detail for different combination of rail-pad stiffness. Low travelling speed (40 km/h) and medium support stiffness (100 MN/m) are considered. Neglecting the imposed constraints in the following considerations, it is possible to minimise the ballast pressure which is associated with track settlement, the excessive contact patch energy (linked with wear and RCF) and the rail-pad forces (linked with component fatigue) with the softest pads, while the stresses on the rail head and foot (linked with component fatigue) with the stiffest pads. The maximum achievable reductions vary from 5% to 20%.

Due to the evident complexity of the objective function, the scope has been restricted to the ballast degradation, considering only the ballast pressure as a major driver of this degradation mode. It has been demonstrated how it is possible to drastically improve the crossing performances finding the optimum value of pad stiffness, in some cases reaching 20% reduction. Each speed and each type of support has different requirements and, therefore, it is not possible to find a unique solution. As general rule, if the line type is slow, it is possible to use soft/medium pads, while if the speed increases it is better to use medium pads.

As further works, it is necessary to include the indicators for the other degradation modes considered (Paragraph 4.1.1). Therefore, relating the weighting factors to the economic impact each degradation mode has in term of maintenance and renewal is crucial. The influence of modelling sleepers as flexible bodies should be also assessed, including the distribution of the support stiffness along the lateral direction. Finally it is a valuable to evaluate the effect of USPs as effective way to enhance the crossing performances.

Acknowledgment

The present work has been supported by the European Commission within the FP7 Capacity4Rail project [Project n. 605650].

References

1. Kassa, E., C. Andersson, and J.C.O. Nielsen, *Simulation of dynamic interaction between train and railway turnout.* Vehicle System Dynamics, 2006. **44**(3): p. 247-258.
2. Nicklisch, D., et al., *Geometry and stiffness optimization for switches and crossings, and simulation of material degradation.* Proceedings of the Institution of Mechanical Engineers, Part F: Journal of Rail and Rapid Transit, 2010. **224**(4): p. 279-292.
3. Markine, V.L., M.J.M.M. Steenbergen, and I.Y. Shevtsov, *Combatting RCF on switch points by tuning elastic track properties.* Wear, 2011. **271**(1–2): p. 158-167.

4. Knothe, K.L. and S.L. Grassie, *Modelling of Railway Track and Vehicle/Track Interaction at High Frequencies.* Vehicle System Dynamics, 1993. **22**(3-4): p. 209-262.
5. Grossoni, I., et al., *Dynamics of a vehicle–track coupling system at a rail joint.* Proceedings of the Institution of Mechanical Engineers, Part F: Journal of Rail and Rapid Transit, 2015. **229**(4): p. 364-374.
6. Kalker, J.J., *Wheel/rail rolling contact theory.* Wear, 1991. **144**: p. 19.
7. Shen, Z.Y., J.K. Hedrick, and J.A. Elkins, *A comparison of alternative creep force models for rail vehicle dynamic analysis.* Vehicle System Dynamics, 1983. **12**(1-3): p. 5.
8. Hunt, G.A., *EUROBALT: vertical dynamic model for track damage studies*. 1998, British Rail Research: Derby.
9. Kaewunruen, S. and A.M. Remennikov, *Sensitivity analysis of free vibration characteristics of an in situ railway concrete sleeper to variations of rail pad parameters.* Journal of Sound and Vibration, 2006. **298**(1–2): p. 453-461.
10. Demharter, K., *Setzungsverhalten des Gleisrostes unter vertikaler Lasteinwirkung*. 1982: Prüfamt für Bau von Landverkehrswegen d. Techn. Univ. München.
11. Guerin, N., *Approche expérimentale et numérique du comportement du ballast des voies ferrées*. 1996, Ecole Nationale des Ponts et Chaussées.
12. Sato, Y., *Japanese Studies on Deterioration of Ballasted Track.* Vehicle System Dynamics, 1995. **24**(sup1): p. 197-208.
13. Evans, J., T. Lee, and C. Hon, *Optimising the wheel/rail interface on a modern urban rail system.* Vehicle System Dynamics, 2008. **46**(S1): p. 119-127.